

## Photocatalytic Decomposition of Nonylphenol in Aqueous Solutions by ZnO Nanoparticles

A.A. BABAIE\*†, A.H. MAHVI\*†, A.R. MESDAGHINIAI, R. NABIZADEH,  
N. JAAFARZADEH HAGHIGHI‡ and F. VAEZI

*Department of Environmental Health Engineering and Center for Environmental Research,  
School of Public Health, Tehran University of Medical Sciences, Tehran, Iran  
Fax: (98)(21)66462267.; Tel: (98)(21)88954914; E-mail: ahmahvi@yahoo.com*

The fundamentals of the photocatalysis based degradation of low concentrations of nonylphenol (NP) an endocrine disrupting compound in batch photoreactor with a UV-visible (UV-Vis) lamp (125 W) and in the presence of ZnO nanocatalyst, under initially environmental conditions and purging oxygen are discussed in this work. The objective of the study is to quantitatively verify the feasibility of nonylphenol degradation with UV-vis/ZnO under such conditions. The conclusions may be potentially helpful to further develop an effective *in situ* treatment of nonylphenol-contaminated water. Initial nonylphenol concentrations ( $[NP]_0$ ) of 100 to 2000 ppb (*ca.* 0.454 to 9.08  $\mu\text{M}$ , respectively) were treated with UV-vis/ZnO using different nano-catalyst loading rates. UV-vis illumination alone degraded insignificant amount of nonylphenol, with negligible changes in total organic carbon, whereas in the presence of ZnO, much faster photodegradation of nonylphenol and effective mineralization occurred;  $99.4 \pm 0.45\%$  and  $93.4 \pm 1.2\%$  of initial nonylphenol was degraded within 2 h in the experiment at  $[NP]_0 \approx 0.454 \mu\text{M}$  and  $[NP]_0 \approx 9.08 \mu\text{M}$ , respectively. The degradation rate constant decreased with an increase in the initial concentration of nonylphenol, while it increased with oxygen concentration. The degradation rate also increased with ZnO loading until a concentration of  $0.5 \text{ g L}^{-1}$ . The degradation rate increased between pH 3.6 and 10, but significantly decreased with increasing pH between 10 and 11.5.

**Key Words:** Photocatalytic degradation, ZnO nano-catalyst, Nonylphenol, Water.

### INTRODUCTION

Low concentration contamination from nonylphenolic compounds is almost omnipresent in the environment. Nonylphenol (NP), which has numerous isomers, is of particular concern because it is persistent, toxic to aquatic organisms and a potential endocrine disruptor. Effects on human and ecosystem health due to low

†National Institute of Health Research, Ministry of Health, Tehran, Iran.

‡Department of Environmental Health, School of Public Health, Jundishapur University of Medical Sciences, Ahvaz, Iran.

concentration exposure to nonylphenol are poorly understood and open to considerable argument. Nonylphenol, an endocrine disrupter and xenobiotic compound from sewage disposal plants, show estrogenic activities at very low concentrations (ppb level) and their feminizing effect on fish is a serious problem in terms of ecological system conservancy<sup>1,2</sup>.

Currently the EPA has accepted the risks of nonylphenol and has prepared a guideline for ambient water quality that recommends nonylphenol concentrations in freshwater be below 6.6 µg/L and in saltwater, below 1.7 µg/L<sup>3</sup>. A maximum acceptable concentration of nonylphenol proposed to be safe and to prevent any toxicity effects on aquatic organisms was 10 µg/L<sup>4</sup>.

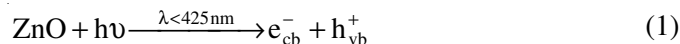
The problem of pollutants, particularly the serious environmental impact of their residues and the relatively low efficiency of the current remediation process, has led to several efforts to elucidate more efficient degradation alternatives. Many works have attempted to degrade numerous pollutants by advanced oxidation processes (AOPs)<sup>5,6</sup>, rather than by other treatment processes. Therefore, in recent years alternative to conventional methods. The advanced oxidation processes (AOPs), based on the generation of highly reactive species such as hydroxyl radicals, which can oxidize a wide range of organic pollutants quickly and non-selective have been developed<sup>7,8</sup>.

Nonylphenols has been found with a concentration of up to 289 µg/L in STP effluents, up to 644 µg/L in natural waters, more than 47.5 mg/L in the industrial STP effluents<sup>9</sup> and even more than 3520 mg/kg and 2530 mg/kg in the sediments and sewage sludge, respectively<sup>10</sup>.

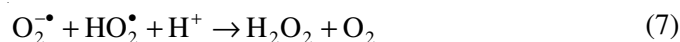
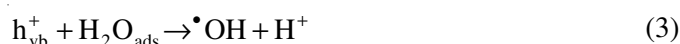
Recently, removal of aqueous nonylphenols by electrochemical<sup>11</sup>, ozonization<sup>11-13</sup>, photolysis with UV<sup>14,15</sup>, photocatalysis with UV/TiO<sub>2</sub> and UV/BiVO<sub>4</sub><sup>16-20</sup> and sonolysis with Fe(II) and Fe(III)<sup>21</sup> has been reported.

However, photocatalysis with UV/ZnO, one of the most promising advanced oxidation processes for the destruction of aquatic pollutants, has not been reported for the degradation of nonylphenols. One of the most important aspects of environmental photocatalysis is the selection of semiconductor materials such as ZnO and TiO<sub>2</sub>: two ideal photocatalysts in several respects. For example, they are relatively inexpensive and they provide photogenerated holes with high oxidizing power due to their wide band gap energy. Since ZnO has nearly the same band gap energy (3.2 eV) as TiO<sub>2</sub>, its photocatalytic capacity is anticipated to be similar to that of TiO<sub>2</sub>. The greatest preference of ZnO in comparison with TiO<sub>2</sub> is that it absorbs over a larger fraction of the UV spectrum and the corresponding threshold of ZnO is 425 nm<sup>22</sup>. For this reason, ZnO photocatalyst is the most suitable for photocatalytic degradation in the presence of sunlight.

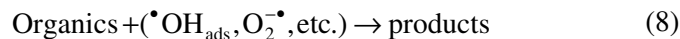
Reaction mechanisms of photocatalytic processes have been discussed extensively in the literature<sup>23-28</sup>. Briefly, illumination of aqueous ZnO suspension with irradiation energy greater than the band gap energy ( $E_{bg}$ ) of the semiconductor ( $h\nu > E_{bg} = 3.2 \text{ eV}$ ) generates valence band holes ( $h^+_{vb}$ ) and conduction band electrons ( $e^-_{cb}$ ) (eqn. 1):



These electron-hole pairs can either recombine (eqn. 2) or interact separately with other molecules. The holes at the ZnO valence band can oxidize adsorbed water or hydroxide ions to produce hydroxyl radicals (eqns. 3 and 4). Electrons in the conduction band can reduce molecular oxygen to superoxide anions ( $\text{O}_2^{\bullet-}$ ) (eqn. 6)<sup>29</sup>.



Produced hydroxyl radicals ( $\bullet\text{OH}_{\text{ads}}$ ) along with other oxidants, *e.g.*, superoxide radical anion ( $\text{O}_2^{\bullet-}$ ), can further mineralize organic compounds to end products (water and  $\text{CO}_2$ ).



In this work, photodegradation of nonylphenol in aqueous ZnO suspension using UV-visible illumination was studied to determine optimal removal conditions with respect to pH, catalyst loading, initial concentrations of nonylphenol, oxygen concentration and illumination time. Variations in the concentration of nonylphenol and total organic carbon (TOC), as well as analysis of kinetic data, were obtained under optimized reaction conditions.

## EXPERIMENTAL

Nonylphenol with purity of 99.5 % was obtained from Dr. Ehrenstorfer-Schafers (Germany). ZnO, NaOH,  $\text{H}_2\text{SO}_4$  were purchased from Merck (Germany) and used without further purification. Solutions were prepared by dissolving required quantity of nonylphenol in double distilled water before each experiment. For the photodegradation of nonylphenol, a solution containing known concentration of the nonylphenol and ZnO nano powder was prepared and it was allowed to equilibrate for 0.5 h in the darkness, then 1 L of the prepared suspension was transferred to the reactor, then the lamp was switched on to initiate the reaction.

**Photocatalytic reaction system:** Photooxidation of nonylphenol was conducted in an annular cylindrical batch reactor with a double layer quartz sleeve at the center of the reactor to house a UV-vis light source. A magnetic stirrer was used to

induce satisfactory mixing of the solution in the reactor. The temperature of the system was maintained at  $26 \pm 0.5$  °C by a quartz cooling water jacket surrounding the quartz sleeve. Depending on the degradation rates under individual reaction conditions, aliquots were sampled and ZnO was separated from suspensions using a centrifuge prior to analysis. Total volume of the withdrawn sample was less than 2 % (by volume) of the solution. To investigate pH effects, pH of the reaction media was adjusted using H<sub>2</sub>SO<sub>4</sub> and NaOH to a desired value throughout the experiments. Oxygen was bubbled into the reaction system to enhance oxygen concentration in the reaction medium, for example up to  $24.4 \pm 0.4$  mg L<sup>-1</sup>, much higher than the saturated value (8.2 mg L<sup>-1</sup> at 26 °C). Temperature, pH (using Metrohm 744 pH-meter, Switzerland) and oxygen concentration (using Winkler method) of reaction media were measured throughout each experiment. Non-porous ZnO (Merck, Germany) with primary particle diameter of 24-71 nm was used as the catalyst. Illumination was performed with UV-visible medium pressure mercury lamp (125 W,  $\lambda_{\text{max}} = 360$  nm), which was placed in central of the quartz sleeve. The UV-visible light intensity in the vicinity of the bulk solution was measured at the external quartz sheath surface and internal reactor surface using a digital UVA radiometer (model EC1 UV-A, Hagner, Bosham, UK). The average intensity of illumination at  $\lambda > 300$  nm was 9.3 mW cm<sup>-2</sup>.

**Chemical analysis:** Nonylphenol was analyzed using a Shimadzu 10Avp series high performance liquid chromatography system (Shimadzu, Japan) coupled with a RF-10A<sub>XL</sub> programmable fluorescence detector. HPLC separations were performed using a Kromasil 100 C<sub>18</sub> column (4.6 mm × 150 mm, 5 μm) from Eka Chemicals AB (Bohus, Sweden) thermostatted at 40 °C, injection volumes of 20 μL, flow rate of 2 mL/min and isocratic elution with 40 % water and 60 % acetonitrile during 25 min. Analytes were monitored by fluorescence detection ( $\lambda_{\text{ex}}$ : 222 nm,  $\lambda_{\text{em}}$ : 305 nm) and quantified by external calibration using peak area measurements. The extent of nonylphenol mineralization was determined through total organic carbon analysis using a Shimadzu model TOC-V<sub>CSH</sub> analyzer (Shimadzu, Japan).

## RESULTS AND DISCUSSION

**Effects of ZnO loading:** ZnO dosage in slurry photocatalytic processes is an important factor that can influence strongly the degradation of the organic substances. The optimum quantity depends on the nature of the organic compound, as well as the photoreactor's geometry<sup>30</sup>. The effect of varying the quantity of ZnO on the observed initial reaction rate of the nonylphenol degradation is illustrated in Fig. 1, which shows that the degradation rate of nonylphenol increased with ZnO loading and reached a plateau at a ZnO loading of 0.5 g L<sup>-1</sup> and decreased slightly beyond 2.0 g L<sup>-1</sup>. As the ZnO concentration increases from 0.1 to 0.5 g L<sup>-1</sup>, the initial reaction rate increases by a factor of 2.47. The curve is reminiscent of a Langmuir-type isotherm, suggesting that the  $r_0$  of the photooxidation reaches a saturation value at higher ZnO concentrations, as has also been reported in similar

cases. This observation can be elucidated in terms of availability of active sites on the catalyst surface and the penetration of UV light into the suspension<sup>31</sup>. Additionally, at a larger catalyst loading, more of the originally activated ZnO may be deactivated through collision with ground-state catalysts<sup>32</sup>. Since agglomeration and sedimentation of ZnO under large catalyst loadings would also take place<sup>33,34</sup>, available catalyst surface for photon absorption would definitely decrease, causing minor increase in the degradation rate beyond an optimum ZnO dosage, 0.5 g L<sup>-1</sup> in this research.

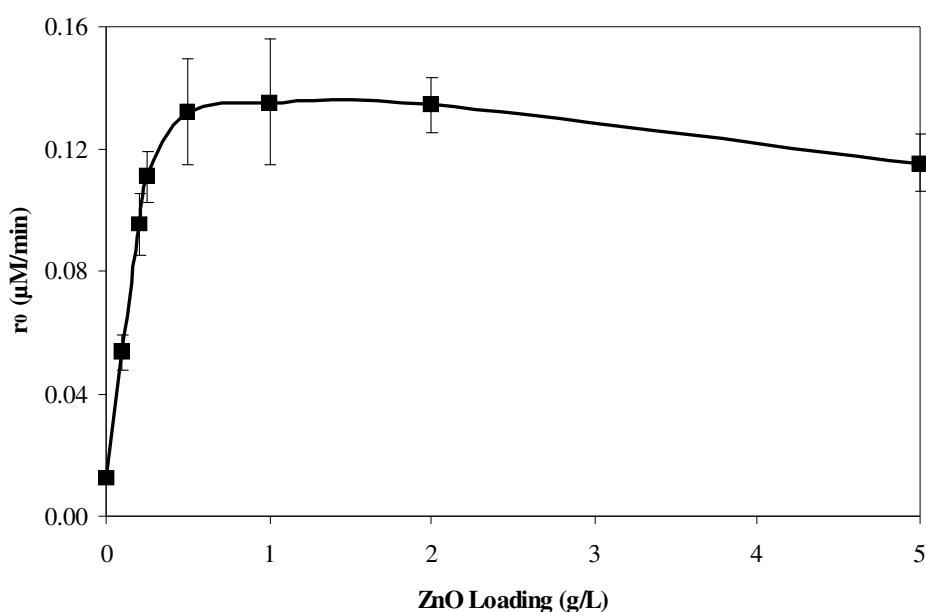


Fig. 1. Effects of ZnO loading on the photocatalytic degradation of nonylphenol with an initial concentration of 4.54  $\mu\text{M}$  (initial pH  $\approx$  7.5)

**Effects of UV-vis light:** Fig. 2 shows the degradation of nonylphenol with an initial concentration of 4.54  $\mu\text{M}$  under three reaction situations. It is noted here that, ZnO and UV-vis alone degraded an insignificant amount of nonylphenol, whereas UV-vis/ZnO successfully degraded nonylphenol. In addition to photolysis under UV-vis illumination, nonylphenol could also be oxidized by  $\cdot\text{OH}$ , which were generated from the reaction between a small portion of UV and water molecules. However, in the presence of ZnO, the direct photolysis can be suppressed due to turbidity and use of photons to activate ZnO. However, in the presence of ZnO with UV-vis illumination, much faster degradation of nonylphenol occurred compared to reactions without ZnO and illumination only. For example, under the same light source, the reaction rate in the presence of ZnO is more than 10 times faster than that in the absence of ZnO.

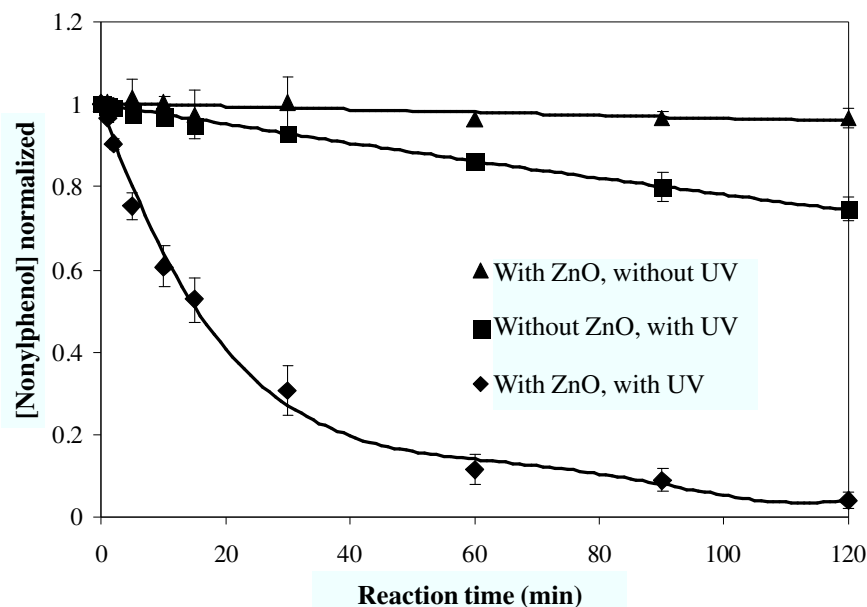


Fig. 2. Photocatalytic degradation of nonylphenol ( $4.54 \mu\text{M}$ ) using three reaction conditions: (▲) with ZnO ( $0.5 \text{ g L}^{-1}$ ), without illumination (initial pH, 7.21-7.57); (■) without ZnO, with UV-vis (initial pH, 7.32-7.73); (◆) with ZnO ( $0.5 \text{ g L}^{-1}$ ), with UV-vis (initial pH, 7.29-7.75)

To monitor the degree of mineralization during photolysis and photocatalytic oxidation of nonylphenol, total organic carbon was tested as shown in Fig. 3. Without any ZnO, although more than 28 % of nonylphenol was removed under UV-vis illumination, equivalent total organic carbon exhibited negligible change by 2 h, indicating low mineralization of nonylphenol intermediates by UV-vis irradiation alone *vice versa* the presence of both ZnO and UV-vis successfully mineralized about 76-95 % of total organic carbon in 2 h. Total organic carbon reduction was reciprocally proportional to  $[\text{NP}]_0$  as indicated in Fig. 3, which shows the total organic carbon reduction after 2 h of reaction, normalized with respect to the  $[\text{TOC}]_0$ . Total organic carbon reduction (at  $t = 2 \text{ h}$ ) showed linear correlations ( $r^2 = 0.977$ ) with  $[\text{NP}]_0$  as shown in Fig. 3.

**Effects of initial nonylphenol concentrations:**  $[\text{NP}]_0$  of 100 to 2000 ppb (*ca.*  $0.454$  to  $9.08 \mu\text{M}$ ) were used for this set of experiments. An optimal ZnO loading rate of  $0.5 \text{ g L}^{-1}$  was selected and the pH was adjusted at *ca.* 7.5. As expected in Fig. 4, nonylphenol degradation was enough high. After 2 h of reaction,  $[\text{NP}]_0$  was degraded by  $99.4 \pm 0.45 \%$  and  $93.4 \pm 1.2 \%$  in the experiment at  $[\text{NP}]_0 \approx 0.454 \mu\text{M}$  and  $[\text{NP}]_0 \approx 9.08 \mu\text{M}$ , respectively. As mentioned before mineralization values reached *ca.* 76 to 95 %, for different  $[\text{NP}]_0$  (Fig. 3). Fig. 5 shows that the first-order degradation rate constant of nonylphenol (solid line) decreased when the initial concentrations of nonylphenol increased from  $0.454$  to  $9.08 \mu\text{M}$  (Table-1).

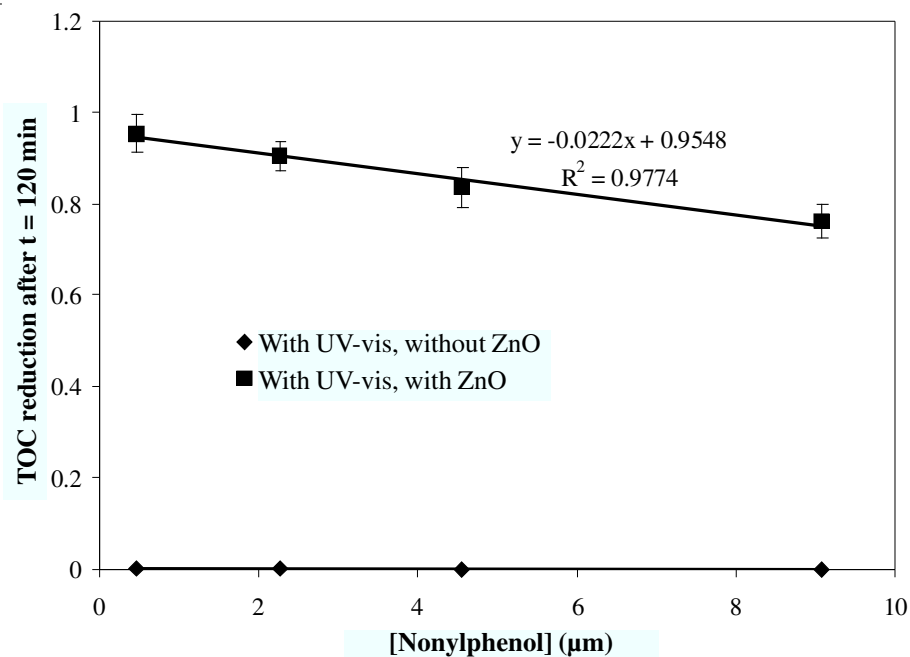


Fig. 3. Effect of  $[NP]_0$  on the degradation of nonylphenol with UV-vis illumination and UV-vis/ZnO process: Total organic carbon reduction variation as function of  $[NP]_0$  (initial pH  $\approx$  7.5 and ZnO loading, 0.5 g L<sup>-1</sup>)

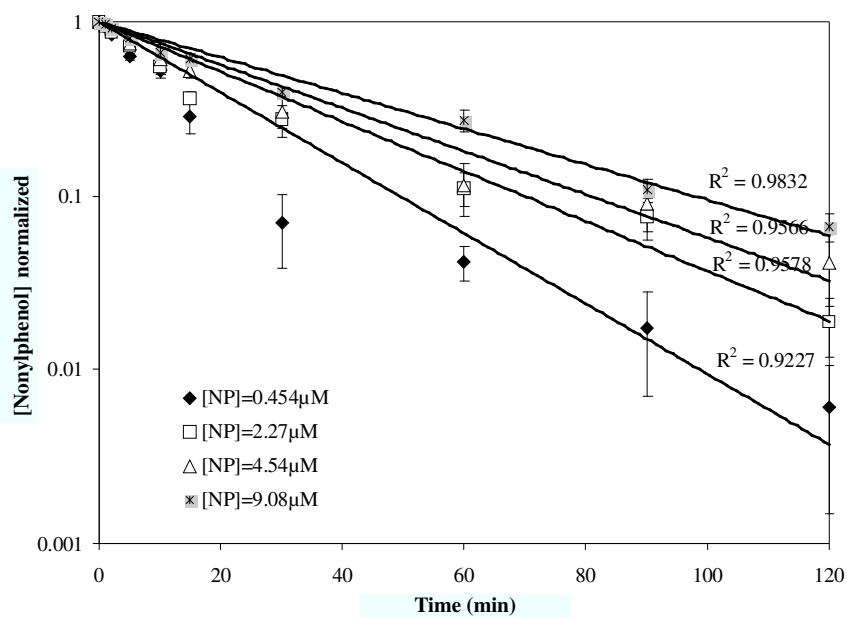


Fig. 4. Effect of  $[NP]_0$  on the degradation of nonylphenol with ZnO loading of 0.5 g L<sup>-1</sup> and initial pH  $\approx$  7.5

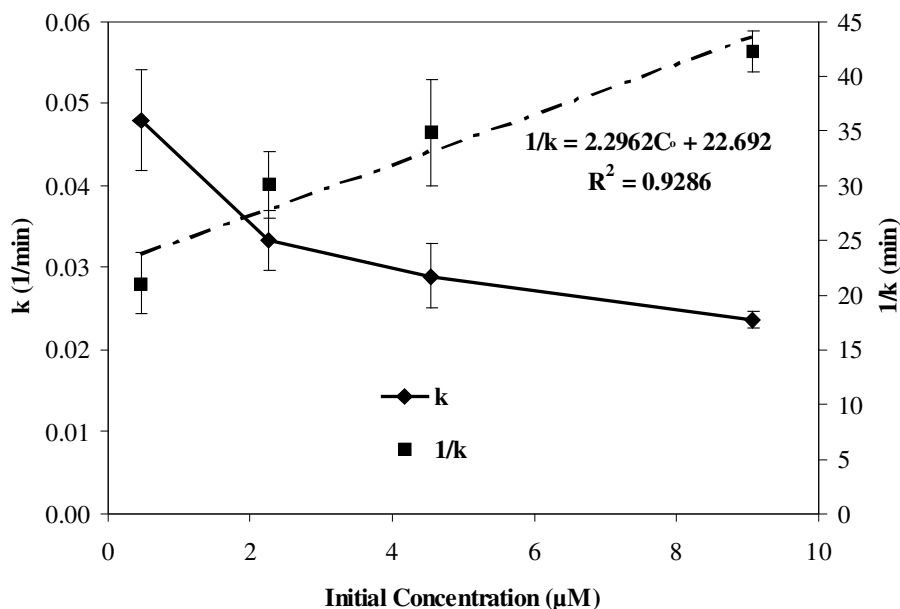


Fig. 5. Effects of initial concentrations of nonylphenol on photocatalytic degradation rate constants ( $k$ ) with ZnO loading of  $0.5 \text{ g L}^{-1}$  (solid line) (initial pH, 7.29-7.75).

TABLE-1  
FIRST-ORDER KINETIC VALUES FOR NP DEGRADATION  
WITH UV-VIS/ZnO AT DIFFERENT  $[\text{NP}]_0$   
(Initial pH  $7.52 \pm 0.23$ , ZnO loading rate  $0.5 \text{ g L}^{-1}$ , reaction time 2 h and  
DO concentration  $5.5 \pm 0.4 \text{ mg L}^{-1}$ )

| $[\text{NP}]_0$ ( $\mu\text{M}$ ) | 0.454             | 2.27                | 4.54               | 9.08                |
|-----------------------------------|-------------------|---------------------|--------------------|---------------------|
| $k$ ( $\text{min}^{-1}$ )         | $0.048 \pm 0.006$ | $0.0334 \pm 0.0036$ | $0.0291 \pm 0.004$ | $0.0237 \pm 0.0011$ |
| $R^2$                             | 0.93              | 0.96                | 0.96               | 0.98                |

At a higher initial concentration, two factors could impede the degradation of nonylphenol; at first, increased amount of nonylphenol may cover a greater number of ZnO active sites, which afterwards suppresses generation of the oxidants (eqns. 3, 4 and 6) and results in lower degradation rates. Secondly, a higher nonylphenol concentration absorbs more photons, consequently decreasing available photons to activate ZnO. Thus, an insufficiency of photons to activate ZnO surface basically retarded the degradation of nonylphenol at a high initial concentration. Hence, the overall reaction rates were lowered with the higher initial nonylphenol concentration. This has been observed in many photochemical reactions where activation by photon absorption is typically the first step for reaction.

**Kinetics of photocatalytic degradation of nonylphenol:** The photocatalytic degradation of nonylphenol with ZnO obscure apparently first order kinetics at low initial nonylphenol concentration and the rate expression is given by eqn. 9.

$$\ln \frac{[\text{NP}]}{[\text{NP}]_0} = -kt \quad (9)$$

where  $k$  is the first order rate constant ( $\text{min}^{-1}$ ),  $[\text{NP}]$  and  $[\text{NP}]_0$  are the nonylphenol concentration at time ' $t$ ' and ' $t = 0$ ', respectively. Table-1 reports the values of  $k$  resulting from plot of  $\ln (C/C_0)$  versus ' $t$ ' for photocatalytic degradation of nonylphenol, which decreases as the initial reactant concentration increases.

A variety of models have been derived to describe the kinetics of photocatalysis, but the most commonly used model is the Langmuir-Hinshelwood (L-H) kinetic model<sup>31,35</sup>. The simplest form of L-H model is summarized as follows:

$$k = \frac{K_{\text{NP}}k_c}{1 + K_{\text{NP}}[\text{NP}]_0} \quad (10)$$

The above equation can be linearized to obtain:

$$\frac{1}{k} = \frac{1}{k_c} \cdot [\text{NP}]_0 + \frac{1}{k_c K_{\text{NP}}} \quad (11)$$

where  $k$  is the first-order rate constant,  $k_c$  is the rate constant of surface reaction ( $\mu\text{M min}^{-1}$ ) and  $K_{\text{NP}}$  is the L-H adsorption constant of NP over ZnO surface ( $\mu\text{M}^{-1}$ ) in aqueous environments. An admissible linear correlation ( $R^2 = 0.9286$ ) between  $1/k$  and  $[\text{NP}]_0$  given in Fig. 4 (dashed line corresponding to the secondary y-axis) indicates that significant adsorption of nonylphenol on ZnO. Surface reactions of nonylphenol, such as oxidation by surface, are important<sup>36</sup>.  $k_c$  and  $K_{\text{NP}}$  were obtained as  $0.4355 \mu\text{M min}^{-1}$  and  $0.1012 \mu\text{M}^{-1}$ , respectively. Since degradation of nonylphenol primarily occurred on the ZnO surface, minimizing the electron-hole pair recombination would accelerate photocatalysis of NP. An efficient trapping of electrons enables reactions of valence band holes ( $h^+_{\text{vb}}$ ) with species adsorbed over the ZnO surface (eqns. 3-5).

Fig. 6 shows the theoretically calculated vs. experimentally obtained first-order rate constants. The calculated data show good agreement with the experimental data ( $R^2 = 0.884$ ).

**Effects of oxygen concentrations:** Presence of electron acceptors is advocated so as to prevent the recombination reaction between the generated positive holes and electrons (eqn. 6)<sup>37-39</sup>. As rule aeration is used for this intention as it also provides uniform mixing, suspension of the catalyst in the case of slurry reactors and economical source of oxygen. Fig. 7 shows that with  $[\text{NP}]_0$   $4.54 \mu\text{M}$  an addition of oxygen of  $24.4 (\pm 0.4) \text{ mg L}^{-1}$  significantly increased the photocatalytic degradation rate of nonylphenol up to more than two times at compared to initial oxygen of  $5.5 \text{ mg L}^{-1}$ , corresponding to the reaction rate constant changing from  $2.9 \times 10^{-2}$  to  $6.0 \times 10^{-2} \text{ min}^{-1}$ . Effects of oxygen concentration on the degradation of nonylphenol could be described using noncompetitive Langmuir kinetic<sup>31,36</sup> equation as:

$$k = k_{\text{O}_2} K_{\text{O}_2} \frac{[\text{O}_2]}{1 + K_{\text{O}_2} [\text{O}_2]}$$

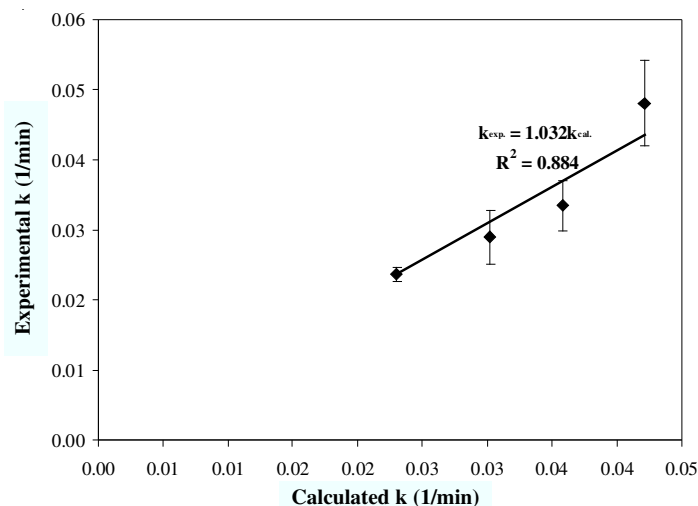
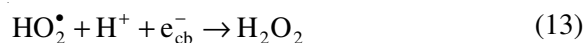


Fig. 6. Comparison between experimental and calculated first-order rate constants for the photocatalytic oxidation of nonylphenol at initial pH 7.29-7.75 and ZnO loading rate 0.5 g L<sup>-1</sup>

where  $k$  is the first-order rate constant,  $k_{O_2}$  is the intrinsic rate constant (mg L<sup>-1</sup> min<sup>-1</sup>) of nonylphenol reaction and  $K_{O_2}$  is Langmuir adsorption constant of oxygen over ZnO surface (mg<sup>-1</sup> L). The noncompetitive Langmuir kinetic equation can be linearized as:

$$\frac{1}{k} = \frac{1}{k_{O_2} K_{O_2}} \cdot \frac{1}{[O_2]} + \frac{1}{k_{O_2}}$$

A plot of the  $1/k$  against  $1/[O_2]$  results in a satisfactory linear correlation ( $R^2 = 0.975$ ), indicating that introducing oxygen into the reaction system effectively inhibits electron-hole recombination as oxygen consumes conduction band electrons, allowing valence band holes to directly (eqn. 5) and indirectly oxidize nonylphenol (eqns. 3, 4 and 8). Based on the intercept and slope of the fitted curve,  $k_{O_2}$  and  $K_{O_2}$  were obtained as  $9.49 \times 10^{-2}$  mg L<sup>-1</sup> min<sup>-1</sup> and  $8.06 \times 10^{-2}$  mg<sup>-1</sup> L, respectively. It is worth noting that oxygen reacting with conduction band electrons forms superoxide radical anion ( $O_2^{\bullet-}$ ) (eqn. 6), which could also directly degrade nonylphenol (eqn. 8). In addition, superoxide radical anion can undergo further reactions and produce  $H_2O_2$  (eqns. 12 and 13), one of the important precursors of generating  $\bullet OH$  (eqns. 14 and 15). Hence, through enhancing  $\bullet OH$ -NP oxidation, superoxide can indirectly degrade nonylphenol:



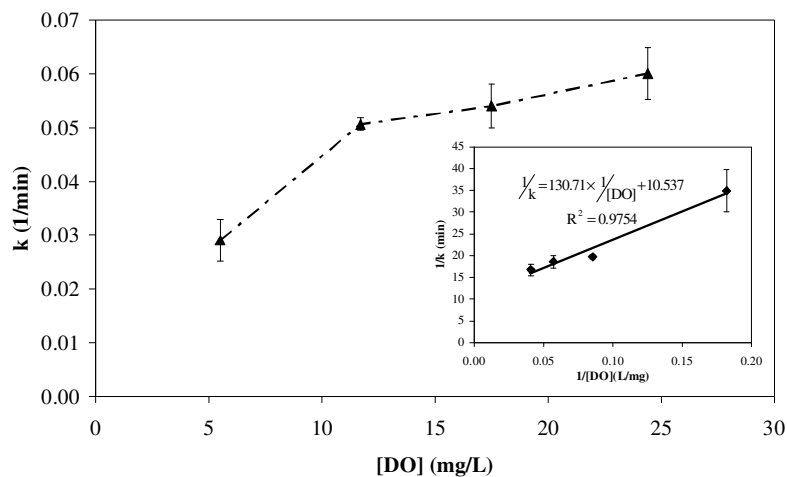


Fig. 7. Effects of oxygen concentration on photocatalytic degradation rate constants ( $k$ ) of nonylphenol with a ZnO loading of  $0.5 \text{ g L}^{-1}$ . The inset represents the relationship between  $1/k$  and  $1/[O_2]$

**Effect of pH:** Medium pH has a complex effect on the rates of photocatalytic oxidation and the observed effect is generally dependent on the type of the pollutant as well as the zero point charge (zPc) of the semiconductor used in the oxidation process, *i.e.* more specifically on the electrostatic interaction between the catalyst surface and the pollutant. The effect of pH on nonylphenol degradation rate was studied by keeping all other experimental conditions fixed and changing the initial pH value of the nonylphenol solution from 3.6 to 11.5 and results are illustrated in Fig. 8.

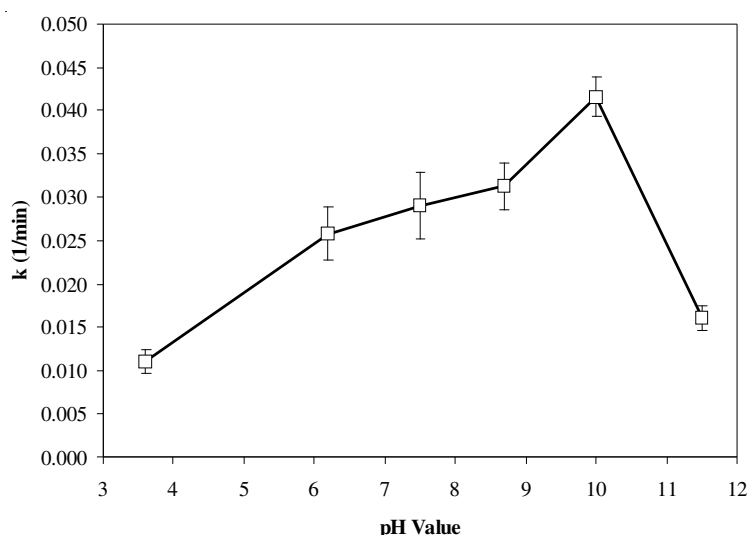
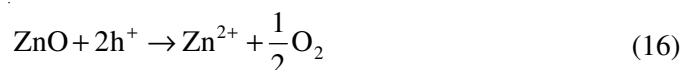


Fig. 8. Effects of pH on the photocatalytic degradation rate constants of nonylphenol with an initial concentration of  $4.54 \mu\text{M}$  and ZnO loading of  $0.5 \text{ g L}^{-1}$ .

The results showed that the degradation rate constant increases with uprising pH up to 10. This can be attributed to enhanced formation of  $\cdot\text{OH}$ , because at high pH (*e.g.*, 10) more hydroxide ions available on ZnO surface can be easily oxidized and form more  $\cdot\text{OH}$  (eqn. 4)<sup>40,41</sup>, which consequently increases the efficiency of nonylphenol degradation. On the other hand, the reaction rate constant significantly decreased at pH 11.5 ( $0.016 (\pm 0.0014) \text{ min}^{-1}$ , Fig. 8), mainly due to surface ionization of ZnO. Since the pHzpc of ZnO is 9.0, the surface of the catalyst is positive below pH 9.0. Again the given dissociation constant (pKa) for nonylphenol is about 10.3<sup>42,43</sup>, therefore nonylphenol is negatively charged above pH 10.3 that might result in electrostatic attraction between the catalyst and nonylphenol and will increase both adsorption and the degree of photodegradation. Regrettably, the mere electrostatic reasoning is unable to entirely account for the relative photocatalytic behaviour as a function of pH. Other co-occurrence effect can come into play. For example ZnO can undergo photocorrosion through self-oxidation (eqn. 16). In particular, ZnO powder display tendency to dissolve with decreasing the pH (eqn. 17). In a strongly alkaline environment, ZnO can undergo dissolution (eqn. 18)<sup>44</sup>.



Therefore, photocatalytic activity of ZnO at exceptionally low and high pH values can be retarded by either acidic/photochemical corrosion of the catalyst (eqns. 16-18) or from alkaline dissolution (eqn. 18). In addition, reactions 16 and 17 can compete with the formation of hydroxyl radicals by decreasing the availability of holes for water or surface  $\text{OH}^-$  oxidation<sup>44</sup> and at a higher pH, the formation of superoxide radical anion ( $\text{O}_2^{\cdot-}$ ) through oxygen reduction by electrons can be suppressed (eqn. 12), which will result in less formation of  $\text{H}_2\text{O}_2$  and  $\cdot\text{OH}$  (eqns. 13-15) and consequently lower the degradation of nonylphenol.

## Conclusion

Nowadays, due to the increasing utilization and presence of recalcitrant, toxic and xenobiotic organic substances in aqueous systems, introduction of newer technologies such as photocatalytic processes, has become imperative. Photocatalytic degradation of nonylphenol in water was studied using nano-catalyst ZnO with UV-vis as light source. It has been found that nonylphenol is readily and rapidly degraded in aqueous solution by UV-vis/ZnO process. The results showed that degradation of nonylphenol was negligible when ZnO nanopowder used without UV-vis light. Although with UV-vis illumination, partially degradation of nonylphenol was found in the absence of ZnO but a minimal change in total organic carbon in 2 h of illumination indicates ineffective mineralization of nonylphenol in the absence of ZnO. A much faster degradation and effective mineralization of nonylphenol took

place under UV-vis illumination in the presence of ZnO. Experimental results showed that the rate constants decrease with an increase in the initial concentration of nonylphenol, but increase with additional oxygen. The reaction rate constants also increased with larger ZnO loading and reached a plateau at ZnO concentration of 0.5 g L<sup>-1</sup> and decreased slightly at a very high concentration of 5.0 g L<sup>-1</sup>. The rate constant increases with increase in pH up to 10, after which a significant decrease is observed. This can be attributed to enhanced formation of <sup>•</sup>OH because at high pH (*e.g.*, 10); however, at pH 11.5, ZnO dissolution retard the degradation of nonylphenol. The kinetics of photocatalytic removal of nonylphenol followed the Langmuir-Hinshelwood model.

### ACKNOWLEDGEMENTS

The authors would like to thank the Research Deputy of Tehran University of Medical Sciences for financial support. The author also gratefully acknowledged Pharmacy Faculty of Jondishapour University of Medical Sciences for their technical assistance.

### REFERENCES

1. K. Inumaru, M. Murashima, T. Kasahara and S. Yamanaka, *Appl. Catal. B: Environ.*, **52**, 275 (2004).
2. USEPA (United States Environmental Protection Agency), **35**, Federal Register 5991 (1990).
3. L. Brooke and G. Thursby, Washington DC, USA: Report for the United States EPA, Office of Water, Office of Science and Technology (2005).
4. K.V. Thomas, M.R. Hurst, P. Matthiessen, D. Sheahan and R.J. Williams, *Water Res.*, **35**, 2411 (2001).
5. M. Lewandowski and D.F. Ollis, *Appl. Catal. B: Environ.*, **43**, 309 (2003).
6. A. Sobczynski, L. Duczmal and W. Zmudzinski, *J. Mol. Catal. A*, **213**, 225 (2004).
7. A. Bozzi, I. Guasaquillo and J. Kiwi, *Appl. Catal. B: Environ.*, **51**, 230 (2004).
8. B. Swarnalatha and A. Anjaneyulu, *J. Mol. Catal. A*, **223**, 161 (2004).
9. M. Auriol, Y. Filali-Meknassi, R.D. Tyagi, C.D. Adams and R.Y. Surampalli, *Process Biochem.*, **41**, 525 (2006).
10. A. Soares, B. Guieysse, B. Jefferson, E. Cartmell and J.N. Lester, *Environ. Int.*, **34**, 1033 (2008).
11. J. Kim, G.V. Korshin and A.B. Velichenko, *Water Res.*, **39**, 2527 (2005).
12. K. Lenz, V. Beck and M. Fuerhacker, *Water Sci. Technol.*, **50**, 141 (2004).
13. B. Ning, N.J.D. Graham and Y. Zhang, *Chemosphere*, **68**, 1163 (2007).
14. M. Neamtu and F.H. Frimmel, *Sci. Total Environ.*, **369**, 295 (2006).
15. P.J. Chen, E.J. Rosenfeldt, S.W. Kullman, D.E. Hinton and K.G. Linden, *Sci. Total Environ.*, **376**, 18 (2007).
16. E. Pelizetti, C. Minero, V. Maurino, A. Sclafani, H. Hidaka and N. Serpone, *Environ. Sci. Technol.*, **23**, 1380 (1989).
17. M. Ike, M. Asano, F.D. Belkada, S. Tsunoi, M. Tanaka and M. Fujita, *Water Sci. Technol.*, **46**, 127 (2002).
18. S. Kohtani, M. Koshiko, A. Kudo, K. Tokumura, Y. Ishigaki, A. Toriba, K. Hayakawa and R. Nakagaki, *Appl. Catal. B: Environ.*, **46**, 573 (2003).
19. S. Kohtani, J. Hiro, N. Yamamoto, A. Kudo, K. Tokumura and R. Nakagaki, *Catal. Commun.*, **6**, 185 (2005).

20. S. Kurinobu, K. Tsurusaki, Y. Natui, M. Kimata and M. Hasegawa, *J. Mag. Magnet. Mat.*, **310**, 1025 (2007).
21. B. Yim, Y. Yoo and Y. Maeda, *Chemosphere*, **50**, 1015 (2003).
22. A. Eslami, S. Nasser, B. Yadollahi, A.R. Mesdaghinia, F. Vaezi, R. Nabizadeh and S. Nazmara, *J. Chem. Technol. Biotechnol.*, **83**, 1447 (2008).
23. M.R. Hoffmann, S.T. Martin, W.Y. Choi and D.W. Bahnemann, *Chem. Rev.*, **95**, 69 (1995).
24. A. Mills and S. Le Hunte, *J. Photochem. Photobiol. A Chem.*, **108**, 1 (1997).
25. D.S. Bhatkhande, V.G. Pangarkar and A.A.C.M. Beenackers, *J. Chem. Technol. Biotechnol.*, **77**, 102 (2002).
26. I.K. Konstantinou and T.A. Albanis, *Appl. Catal. B: Environ.*, **49**, 1 (2004).
27. K. Kabra, R. Chaudhary and R.L. Sawhney, *Ind. Eng. Chem. Res.*, **43**, 7683 (2004).
28. O. Carp, C.L. Huisman and A. Reller, *Prog. Solid State Chem.*, **32**, 33 (2004).
29. M.A. Behnajady, W. Modirshahla, N. Daneshvar and M. Rabbani, *J. Hazard. Mater.*, **140**, 257 (2007).
30. S. Parra, J. Olivero and C. Pulgarin, *Appl. Catal. B: Environ.*, **36**, 75 (2002).
31. N. Daneshvar, M. Rabbani, N. Modirshahla and M.A. Behnajady, *J. Photochem. Photobiol. A Chem.*, **168**, 39 (2004).
32. B. Neppolian, H.C. Choi, S. Sakthivel, B. Arabindoo and V. Murugesan, *J. Hazard. Mater.*, **89**, 303 (2002).
33. C.M. So, M.Y. Cheng, J.C. Yu and P.K. Wong, *Chemosphere*, **46**, 905 (2002).
34. N. San, M. Kilic, Z. Tuiebakhova and Z. Cinar, *J. Adv. Oxid. Technol.*, **10**, 43 (2007).
35. M.A. Behnajady, N. Modirshahla and R. Hamzavi, *J. Hazard. Mater.*, **133**, 226 (2006).
36. D.W. Chen and A.K. Ray, *Water Res.*, **32**, 3223 (1998).
37. H. Shibata, Y. Ogura, Y. Sawa and Y. Kono, *Biosci. Biotechnol. Biochem.*, **62**, 2306 (1998).
38. S. Yamazaki, S. Matsunaga and K. Hori, *Water Res.*, **35**, 1022 (2001).
39. G.R. Bamwenda, T. Uesigi, Y. Abe, K. Sayama and H. Arakawa, *Appl. Catal. A: Gen.*, **205**, 117 (2001).
40. S.R. Zheng, Q.G. Huang, J. Zhou and B.K. Wang, *J. Photochem. Photobiol. A Chem.*, **108**, 235 (1997).
41. C. Galindo, P. Jacques and A. Kalt, *J. Photochem. Photobiol. A Chem.*, **130**, 35 (2000).
42. S. Muller and C. Schlatter, *Pure Appl. Chem.*, **70**, 1847 (1998).
43. P. Ivashechkin, P.F.X. Corvini and M. Dohmann, *Water Sci. Technol.*, **50**, 133 (2004).
44. N. Daneshvar, S. Aber, M. S. Seyed Dorraji, A. R. Khataee and M. H. Rasoulifard, *Int. J. Chem. Biomol. Eng.*, **1**, 28 (2008).